SOLAR WIND MINOR ION CHARGE STATES OBSERVED WITH HIGH TIME RESOLUTION WITH SOHO/CELIAS/CTOF

M.R. Aellig[1], H. Grünwaldt[2], P. Bochsler[1], S. Hefti[1], P. Wurz[1], R. Kallenbach[1], F.M. Ipavich[3], D. Hovestadt[4], M. Hilchenbach[2], and the CELIAS Team

[1] Physikalisches Institut, University of Bern, Bern, Switzerland
[2] Max-Planck-Institut für Aeronomie, Katlenburg-Lindau, Germany
[3] Dept. of Physics and Astronomy and IPST, University of Maryland, College Park, USA
[4] Max-Planck-Institut für extraterrestrische Physik, Garching, Germany

ABSTRACT

The SOHO/CELIAS/CTOF (Charge Time Of Flight) mass spectrometer measures the ionic and elemental composition of minor ions in the solar wind with unprecedented time resolution. As shown by different authors (e.g. Hundhausen 1972, Owocki et al. 1983) the charge states of minor ions in the solar wind provide a powerful tool to detect changes of the electron temperature profile in the solar corona. We apply this well-known method to interpret the SOHO/CELIAS/CTOF data. Due to the high sensitivity of the CTOF sensor we can perform coronal diagnostics using solar wind *in situ* measurements with high time resolution.

We briefly describe the relevant quantities and approximations to determine the freezing of charge states of minor ions. The application of a simple description of the coronal expansion to calculate the freeze-in temperatures results in a parametrization of the latter with coronal properties. The influence of the coronal parameters is discussed. We vary the temperature profile to match the observed freeze-in temperatures. Analysis of extended periods of time shows considerable variations of the temperature profile in the inner corona on short time scales. We discuss the sensitivity of the results to some of the assumptions, such as the electron density and the superradial expansion.

Key words: solar wind; minor ions; charge states; coronal temperature profile.

1. INTRODUCTION

In this section the relevant equations and time scales are introduced. For more details we refer to the articles by Hundhausen (1972), and Owocki et al. (1983). In a steadily outflowing solar wind the conservation of particles requires for a given ionization stage i of a species X

$$\nabla(n_i \mathbf{u_i}) = n_e[n_{i-1}C_{i-1} - n_i(C_i + R_i) + n_{i+1}R_{i+1}] \quad (1)$$

where C_i and R_i denote the electron temperature dependent ionization and recombination rate coefficients of the ion X^{i+}. n_e and n_i are the densities of electrons and of the species X^{i+}, respectively. The velocity of the ion X^{i+} is denoted by $\mathbf{u_i}$. Eq. 1 defines the characteristic time for a charge modification of an adjacent pair of ionization stages $i, i+1$ by

$$\tau_{i \leftrightarrow i+1} = \frac{1}{n_e(C_i + R_{i+1})} \quad (2)$$

This characteristic time depends on r, the heliocentric distance, via the electron density n_e and also via the temperature-dependent rate coefficients C_i, R_{i+1}. The characteristic time $\tau_{i \leftrightarrow i+1}$ increases with r in the corona due to the decrease of the electron density and the electron temperature.

The characteristic time scale of the solar wind outflow is the expansion time τ_{exp}, i.e. the time it takes ions to flow through one electron density scale height H. If we assume the speed of a given species X to be independent of its degree of ionization i, i.e. $u_i = u$, the expansion time

$$\tau_{exp} = H/u \quad (3)$$

is also independent of the charge state i unlike $\tau_{i \leftrightarrow i+1}$. The expansion time τ_{exp} is known to decrease in the inner corona (e.g. Hundhausen 1972) because the solar wind is strongly accelerated in this region.

Considering an equilibrium situation rather than the dynamical solar wind outflow the density ratio of adjacent charge states obeys

$$\frac{n_i}{n_{i+1}} = \frac{R_{i+1}(T_e)}{C_i(T_e)} = f_i(T_e) \quad (4)$$

In the following we assume that the density ratio adjusts according to eq. 4 until the solar wind expansion dominates and that it does not change

Proc. 31st ESLAB Symp., 'Correlated Phenomena at the Sun, in the Heliosphere and in Geospace', ESTEC, Noordwijk, The Netherlands, 22-25 September 1997 (ESA SP-415, December 1997)

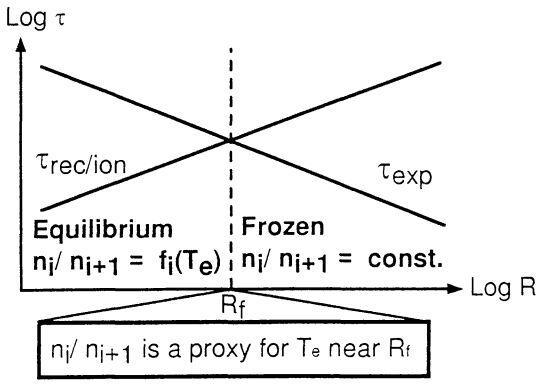

Figure 1. The concept of sudden freezing. As long as the charge modifcation is faster than the expansion of the solar wind, a given density ratio of adjacent charge states is adjusted according to the local electron temperature. Furthermore it is assumed that this density ratio freezes at the location where the expansion time equals the recombination/ionization time.

thereafter. The concept of sudden freeze-in is illustrated schematically in Figure 1. Depending upon the species considered, the freeze-in condition

$$\tau_{i \leftrightarrow i+1} = \tau_{exp} \tag{5}$$

is fulfilled between a fraction of a solar radius and a few solar radii above the solar surface. If the simple concept of sudden freezing were true, we would measure directly the electron temperature T_e at the location R_f where eq. 5 holds for a given ion pair $(i, i+1)$. However, the charge state modification will fade out near the freeze-in radius R_f rather than stop at once. Nevertheless the temperature given by eq. 4 is a proxy of the coronal electron temperature at the freezing point R_f that is derived from eq. 5.

Measuring densities of individual species X^{i+} allows to derive freeze-in temperatures according to eq. 4. In Section 5. these measured values will be compared to a parametrization of the freeze-in temperatures $T_{f,i}$ with the coronal electron temperature profile and the solar wind outflow. This parametrization is presented in Section 3.

2. INSTRUMENT DESCRIPTION

The CTOF sensor of the SOHO/CELIAS experiment is a linear time-of-flight mass spectrometer using the carbon foil technique. It is especially designed to separate the individual charge states of elements up to Fe and also to distinguish between different species with the same mass per charge such as Fe^{14+} and Si^{7+}. A more detailed description of the sensor is given by Hovestadt et al. (1995).

The densities of the different iron charge states have been derived based on an instrument response model and on a maximum likelihood inversion algorithm developed by Aellig (1998) whereas the densities of the oxygen ions have been determined by Hefti (1997). In both cases so-called matrix elements have been used that sum the counts accumulated during a full instrument cycle in rectangular regions of the mass and mass per charge domain.

3. PARAMETRIZATION OF CORONAL PROPERTIES

In this section we present a simple parametrization of coronal properties. It will be used as an estimate of coronal parameters based on the measured freezing-in temperatures. The solar wind outflow is described by

$$n_e = n_0 z^a \tag{6}$$
$$T_e = T_0 z^b \tag{7}$$
$$u_i = u_0 z^{-c} \tag{8}$$
$$A = z^{-d} \tag{9}$$

where $z = R_\odot / r$. The electron density is denoted by n_e and the electron temperature by T_e. The speed of the ions u_i is assumed to be independent of the species. The superradial expansion is denoted by A with $d = 0$ corresponding to the case of radial expansion. The conservation of mass requires the exponents a, c, d to satisfy

$$c = a - d - 2 \tag{10}$$

With eq. 6, 8, 10 the solar wind expansion time given by eq. 3 can be calculated. To determine the charge modification time given by eq. 2, the sum of the relevant rate coefficients is parametrized

$$C_i + R_{i+1} = S_{0,i}\, T_e^{\alpha_i} \tag{11}$$

The rate coefficients for the different iron ionization states are given by Arnaud & Raymond (1992) and for oxygen by Arnaud & Rothenflug (1985).

Applying the conditions of sudden freeze-in we can calculate the freeze-in radius $R_{f,i}$ for a pair of ions $X^{i+}, X^{(i+1)+}$ by solving eq. 5.

$$R_{f,i} = R_\odot \left(\frac{R_\odot n_0 S_{0,i} T_0^{\alpha_i}}{a\, u_0} \right)^{\frac{1}{2a-3-d+\alpha_i b}} \tag{12}$$

As stated above we assume that the measured freezing-in temperature equals the electron temperature at the freezing radius, i.e. $T_{f,i} = T_e(R_f)$.

$$T_{f,i} = \frac{T_0^{\left(1-\frac{\alpha_i b}{2a-3-d+\alpha_i b}\right)}}{\left(\frac{R_\odot n_0 S_{0,i}}{a u_0}\right)^{\frac{b}{2a-3-d+\alpha_i b}}} \tag{13}$$

It will turn out that $T_{f,i}$ is strongly determined by the parameter T_0 since it depends on the latter with an exponent close to unity whereas the coronal base values of the electron density n_0 and the solar wind velocity u_0 appear with a small exponent in the denominator in eq. 13.

Because the reaction rates vary strongly with different species, we can determine the electron temperature at different locations $R_{f,i}$ and thus also fit the logarithmic gradient of the electron temperature, i.e. the parameter b. Taking the logarithm of eq. 13 and building the difference for two ion pairs we get for b

$$b = (2a - d - 3)\frac{\ln\left(\frac{T_{f2}}{T_{f1}}\right)}{\ln\left(\frac{T_{f1}^{\alpha_1} S_{0,1}}{T_{f2}^{\alpha_2} S_{0,2}}\right)} \qquad (14)$$

In this parametrization the estimated value for b depends on a which is the exponent for the power law of the the electron density and to a lesser extent on d which is the power law index of the superradial expansion.

4. DATA ANALYSIS

From SOHO/CELIAS/CTOF data we derive by application of eq. 4 the freeze-in temperatures of the ion pairs $O^{6+} \leftrightarrow O^{7+}$, $Fe^{9+} \leftrightarrow Fe^{10+}$, and $Fe^{11+} \leftrightarrow Fe^{12+}$. These temperatures are fitted to eq. 13 by varying the electron temperature profile via the parameters T_0 and b. The values of a, d, and n_0 remain fixed under all solar wind conditions whereas the velocity at the coronal base u_0 is bound linearly to the temperature T_0, i.e. $u_0 = v_0 T_0$.

The oxygen is known to freeze at about $1.5\,R_\odot$ whereas the different iron charge states freeze in the range $3-5\,R_\odot$, thus covering a sufficient range to derive a radial gradient. The O^{6+} ion is generally the most prominent minor ion in the solar wind and its density can therefore be determined accurately. We have chosen the Fe^{10+}/Fe^{9+} ratio to determine its freeze-in temperature because these species are generally the most prominent charge states of iron ions in the solar wind. The Fe^{12+}/Fe^{11+} density ratio can be determined accurately with high time resolution as well and the reaction rates differ more from the Fe^{10+}/Fe^{9+} pair than those of the Fe^{11+}/Fe^{10+} pair do.

The parameters of the electron density are set to $a = 4.9$ and $n_0 = 2.1 \times 10^{14}\,\mathrm{m}^{-3}$ based on a fit to data presented by Guhathakurta et al. (1996). We have assumed a radial solar wind expansion, i.e. $d = 0$ which yields $c = 2.9$ as the power law exponent of the speed, whereas for v_0 a value of 500 m s^{-1} MK^{-1} is adopted. The constants of the reaction rates parametrized according to eq. 11 are summarized in Table 1.

Table 1. Rate coefficient parameters.

Ion pair	α	S_0 [m^3 s^{-1} MK$^{-\alpha}$]
$O^{6+} \leftrightarrow O^{7+}$	1.37	1.10×10^{-18}
$Fe^{11+} \leftrightarrow Fe^{12+}$	0.84	1.46×10^{-16}
$Fe^{9+} \leftrightarrow Fe^{10+}$	1.34	2.33×10^{-16}

5. RESULTS AND DISCUSSION

As outlined in the previous section, the parameters T_0 and b have been fitted to the measured freeze-in temperatures. Using these estimates the freeze-in radii are calculated according to eq. 12. An example of an electron temperature profile determination is shown in Figure 2, where the measured freeze-in temperatures have been smoothed with a boxcar average of 25 minutes width. We note that the temperature steeply decreases with a power law index of $b = 0.75 \pm 0.14$ that differs considerably from the value of the heat conduction dominated corona of 2/7. The parameter T_0 has no direct physical meaning since the temperature profile should not be extrapolated to the solar surface. It is, however, a good indicator for temperature changes near the temperature maximum.

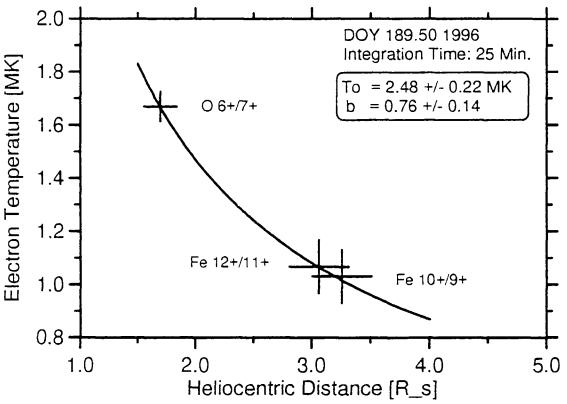

Figure 2. Electron temperature profile determined with a time resolution of 25 minutes. Note the steep decrease of the electron temperature. Estimates of the uncertainties of the freeze-in temperatures are indicated. The uncertainties of the freeze-in radii are calculated with eq. 12 using the laws of error propagation.

An example of a flatter electron temperature profile is shown in Figure 3, where the derived exponent $b = 0.35 \pm 0.11$ is consistent with the value of the heat conduction dominated corona.

In the denominator of eq. 13 the coronal outflow properties n_0 and u_0 enter via their ratio. We have changed the ratio n_0/u_0 by a factor of 5 and fitted the temperature again. The result shows that T_0 increases by about 0.14 MK for this increase of n_0/u_0 whereas it decreases by the same amount if n_0/u_0 is lowered by a factor of 5. Note that the exponent b is insensitive to these changes, i.e. the electron temperature gradient does not depend on the assumptions adopted for n_0/u_0 which is also seen from eq. 14.

In order to assess temporal changes of the temperature profile we have performed the fit not only for two examples but for an extended period of 80 days in 1996. The result is shown in Figure 4 where we display the fitted parameter b and the calculated electron temperature at the freeze-in radius of the ion pair $O^{6+} \leftrightarrow O^{7+}$. In addition the freeze-in radii of

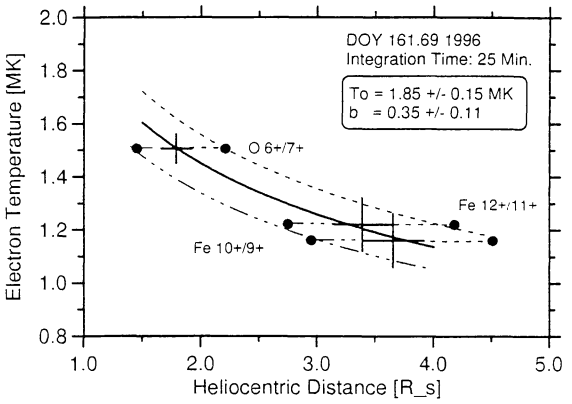

Figure 3. Electron temperature profile determined with a time resolution of 25 minutes. This profile is flatter than the one shown in Figure 2. The dashed line is the result for the ratio n_0/u_0 increased by a factor of 5 relative to the reference value used for the solid line, whereas the dashed-dotted line was calculated with a ratio that was lowered by a factor of 5. The dots indicate the measured freeze-in temperatures in cases the ratio n_0/u_0 is changed. Note that the logarithmic gradient of the electron temperature is not affected by these changes.

this ion pair and $Fe^{9+} \leftrightarrow Fe^{10+}$ as well as the solar wind speed derived from SOHO/CELIAS/Proton Monitor data are shown.

Considerable variations of the logarithmic temperature gradient b are observed on short time scales. In this model such changes correlate with the electron temperature at the freeze-in radius of the oxygen pair, T_{76}. The correlation between T_{76} and b is explained by the fact that the oxygen freeze-in temperature varies over a larger range than the iron freeze-in temperatures do. If the oxygen freeze-in temperature increases stronger than the iron freeze-in temperature, it is evident that the temperature gradient b increases as well. We determine a mean value of the gradient of $\bar{b} = 0.49$ assuming radial expansion. From eq. 14 we see that superradial expansion, i.e. $d > 0$, decreases the inferred value of b. If we adopt an exponent $d = 1.5$, the superradial expansion of $A = 8$ at $r = 4\,R_\odot$ is in reasonable agreement with a model of magnetic flux-tube geometry by Wang & Sheeley (1990) but is lower compared to their model closer to the sun. We then estimate the mean value to be $\bar{b}_{d=1.5} = \frac{5.3}{6.8}\,\bar{b} = 0.38$ by application of eq. 14. By inspection of Figure 4 we see that, in general, the lowest values of b are observed for increased solar wind speed, e.g. around DOY 215. This could reflect the fact that the superradial expansion in the inner corona is not a constant [Wang & Sheeley 1990] as assumed for the present analysis but decreases with increasing solar wind speed. Adiabatic expansion in the strongly expanding flux tubes of the very slow solar wind might additionally cool the electrons and explain the excess of the determined value of the parameter b over the 2/7 for the heat conduction dominated corona.

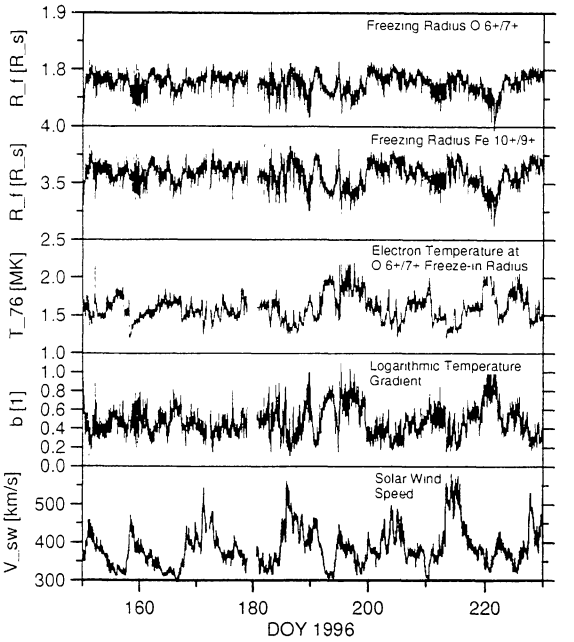

Figure 4. Overview of the logarithmic temperature gradient b and the electron temperature T_{76} at the freeze-in radius of the $O^{6+} \leftrightarrow O^{7+}$ pair. The parameter b varies considerably on short time scales. These variations correlate with T_{76}. The freeze-in radii, shown in the upper panels, depend only weakly on the temperature profile parameters. The lowest panel displays the solar wind speed derived from SOHO/CELIAS/Proton Monitor data.

6. CONCLUSIONS

We have applied the well known concept of charge state freezing of minor ions in the solar wind to detect changes in the coronal electron temperature profile. The application of a simple parametrization of coronal properties on the highly time resolved freeze-in temperatures derived from SOHO/CELIAS/CTOF data shows large variation of the temperature gradient between $r \approx 1.5\,R_\odot$ and $r \approx 3.5\,R_\odot$ on short time scales. In this model large gradients correlate with high coronal temperatures.

ACKNOWLEDGMENTS

This work was supported by the Swiss National Science Foundation and by DARA, Germany.

REFERENCES

Aellig M.R., 1998, PhD Thesis, University of Bern, Switzerland

Arnaud, M., and Rothenflug, R., 1985, Astron. Astrophys. Suppl. Ser., 60, 425

Arnaud, M., and Raymond, J., 1992, ApJ, 398, 394

Guhathakurta, M., Holzer, T.E., and MacQueen, R.M., 1996, ApJ, 458, 817

Hefti, S., 1997, PhD Thesis, University of Bern, Switzerland

Hovestadt, D. et al., 1995, Solar Physics, 162, 441

Hundhausen, A.J., 1972, Coronal expansion and solar wind, Springer Verlag

Owocki, S.P., Holzer, T.E., and Hundhausen, A.J., 1983, ApJ, 275, 354

Wang, Y.-M., and Sheeley Jr., N.R., 1990 ApJ, 355, 726